

Direct observation of the coexistence of pseudogap and superconducting quasi-particles in Bi2212 by time-resolved optical spectroscopy

Y. H. Liu*,¹ Y. Toda,^{2,3} K. Shimatake,^{2,3} N. Momono,⁴ M. Oda,¹ and M. Ido¹

¹*Department of Physics, Hokkaido University, Sapporo 060-0810, Japan*

²*Department of Applied Physics, Hokkaido University, Sapporo 060-0810, Japan*

³*Division of Innovative Research CRIS, Hokkaido University, Sapporo 001-0021, Japan*

⁴*Department of Materials Science and Engineering,*

Muroran Institute of Technology, Muroran 050-8585, Japan

(Dated: October 29, 2018)

We report the ultra-fast optical response of quasi-particles (QPs) in both the pseudogap (PG) and superconducting (SC) states of underdoped (UD) $\text{Bi}_2\text{Sr}_2\text{CaCu}_2\text{O}_{8+\delta}$ (Bi2212) single crystal measured with the time-resolved pump-probe technique. At a probe energy $\hbar\omega_{pr}=1.55$ eV, it is found that the reflectivity change $\Delta R/R$ changes its sign at exactly T_c , which allows the direct separation of the charge dynamics of PG and SC QPs. Further systematic investigations indicate that the transient signals associated with PG and SC QPs depend on the probe beam energy and polarization. By tuning them below T_c two distinct components can be detected simultaneously, providing evidence for the coexistence of PG and SC QPs.

PACS numbers: 68.37.Ef, 74.72.Hs, 74.25.-q, 74.50.+r

The relationship between the anomalous PG state and high- T_c superconductivity is still an important open issue in condensed matter physics. Two main scenarios have been put forward to help us to understand this relationship well within a theoretical framework. One proposes that the PG state is dominated by a hidden order, which competes with high- T_c superconductivity. The other emphasizes that the PG state is a precursor of high- T_c superconductivity. In this picture, high- T_c superconductivity originates from the PG state where Cooper pairs are formed but lack long-range phase coherence, which will be established below T_c . In early research, angle-resolved photoemission spectroscopy (ARPES) and electron tunneling spectroscopy revealed that the PG could smoothly evolve into the SC gap as the temperature fell below T_c , while electronic Raman scattering (ERS) data showed that nodal and antinodal gaps coexisted below T_c [1, 2]. In fact, this discrepancy can be understood well in terms of the scenario of the ‘‘Fermi-arc’’ superconductivity [2], which is supported by additional high-resolution data recently obtained again by ERS [3] and by ARPES [4, 5, 6], revealing that for UD cuprate superconductors below T_c there are two energy scales in the nodal and antinodal regions on the Fermi surface. Such a high consistency of different experimental data validates the contention that the SC gap located in the nodal region, called ‘‘Fermi-arc’’ superconductivity [2, 4, 7, 8, 9], is distinct from the PG located in the antinodal region for UD cuprate superconductors.

Distinguishing the charge dynamics of QPs in the antinodal and nodal regions will be helpful as regards revealing the mechanism responsible for them. Time-resolved pump-probe optical spectroscopy with femto-second resolution is a powerful tool for determining the charge dynamics of carriers in superconductors [10]. In

such measurements, a pump pulse with a higher energy than the SC energy gap breaks Cooper pairs into two electrons (or photoexcited carriers) and excites them to a non-equilibrium high-energy state. Subsequently the probe pulse detects, within the delay time between the pump and probe pulses, the process by which photoexcited carriers recombine into a superconducting condensate. Below T_c , the PG does not change into the SC gap for UD cuprate superconductors [1, 2, 3, 4, 5, 6], meaning that the relaxation process of SC QPs (Cooper pairs) should differ from that of PG QPs. Therefore, in principle this technique can be used to distinguish different relaxation processes involving PG and SC QPs in UD Bi2212 by measuring the sample reflectivity change $\Delta R/R$. Previously pump-probe experiments revealed that $\Delta R/R$ could be either positive or negative [11, 12, 13, 14, 15, 16]. In particular, Mihailovic *et al.* [13, 14, 17, 18] and Murakami *et al.* [15] have already conducted a self-consistent two-component analysis of the optical spectroscopy data obtained by the pump-probe technique, demonstrating that PG QPs coexist with SC QPs below T_c . However, a direct and unambiguous identification of distinct charge dynamics associated with SC and PG QPs still lacks. Recently, we have used two-color time-resolved pump-probe optical spectroscopy to investigate NbSe_3 with two charge-density wave (CDW) transitions occurring at different temperatures [19], revealing that the two transitions can be selectively detected at temperatures far below the CDW transition temperatures. In this letter, we report the direct identification of the charge dynamics of PG and SC QPs by measuring $\Delta R/R$ of the UD Bi2212, using the same technique as that described in Ref. [19].

UD Bi2212 single crystals with $T_c=76$ K (hole concentration 0.11) are grown by the traveling solvent floating

zone method using an infrared image furnace. The time-resolved reflectivity change $\Delta R/R$ is measured by using the pump-probe technique on the sample mounted in a cryostat whose temperature ranges from 4 to 300 K. Both the probe and pump beams are crossed and incident in the c-axis direction on freshly cleaved surfaces. The laser power induced heating effect has been accounted for by measuring the temperature dependence of the $\Delta R/R$ amplitude at different given powers. The pump-probe experimental configurations have been described in detail elsewhere [19].

Figure 1(a) shows the temperature evolution of $\Delta R/R$ as a function of delay time measured at a probe energy $\hbar\omega_{pr}=1.55$ eV and a pump energy $\hbar\omega_{pu}=1.07$ eV over a wide temperature range from 15 to 280 K. This waterfall plot shows that the sign changes of $\Delta R/R$ occur just at the SC transition temperature T_c and the PG-opening temperature T^* , respectively. It should be pointed out that the T^* determined here is consistent with the result of the tunneling spectroscopy [20]. The sign of $\Delta R/R$ below T_c and above T^* is positive, whereas it is negative between T_c and T^* . Hereafter, we define the positive (negative) signal as one with a positive (negative) sign. Using a single-component exponential decay function $\Delta R/R(T, t)=A(T)\exp(-t/\tau)$, where $A(T)$ is the amplitude of $\Delta R/R$ as a function of temperature (T) and τ is the relaxation time of QPs, we can fit the data well [solid lines in Figs. 1(b), (c) and (d)] and achieve the relaxation times for different QPs, whose temperature dependence is shown in Fig. 2(a). Considering the noticeable sign changes of $\Delta R/R$ present at T_c and T^* , we naturally assign the positive component appearing below T_c with a slow decay of ~ 2.5 ps to SC QPs (Cooper pairs), which corresponds to those obtained on $Y_{1-x}Ca_xBa_2Cu_3O_{7-\delta}$ single crystal [14] and UD Bi2212 film [15] using two-component analysis. Another component that appears above T_c and fades out at T^* is ascribed to PG QPs with a relaxation time of ~ 0.5 ps. The third component appearing above T^* is a step-function response with a relaxation time of ~ 0.8 ps [Fig. 1(d)], which is a typically bolometric effect in the metal [21] and similar to that observed in $YBa_2Cu_3O_{7-\delta}$ (Y123) at 300 K [22]. This observation is consistent with ARPES results showing that UD Bi2212 is a metal above T^* [23]. In this letter, we focus our attention on the two components present below T^* . The temperature dependence of the amplitude of $\Delta R/R$ is shown in Fig. 2(b), which shows two features: (1) the amplitude of the positive SC component decreases with increasing temperature and becomes zero at T_c ; (2) the negative PG component starts to appear at T_c and fades out around T^* .

Figures 3(a) and (b) show the effect of the probe beam polarization on $\Delta R/R$ measured at $\hbar\omega_{pr}=1.55$ eV below and above T_c . It is worthwhile noting that $\Delta R/R$ shows no dependence on the pump beam polarization, which

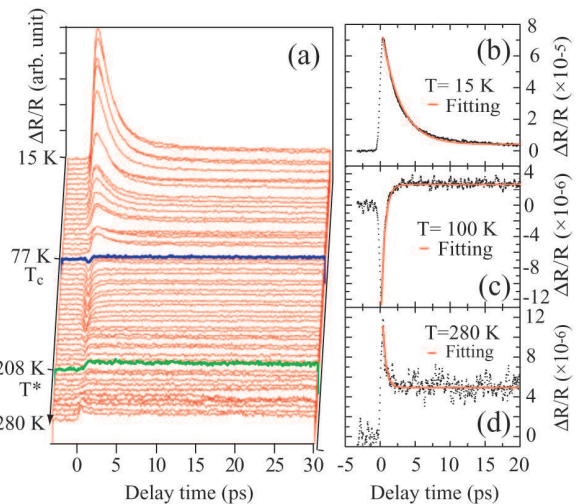


FIG. 1: (Color online) (a) Waterfall plot for $\Delta R/R$ as a function of delay time over a wide temperature range from 15 to 280 K measured at $\hbar\omega_{pu}=1.07$ eV and $\hbar\omega_{pr}=1.55$ eV. The pump and probe beams are polarized at 90° and 0° relative to the b axis, respectively. The sign changes of $\Delta R/R$ at T_c and T^* can be clearly seen. Note that the temperature of each curve corresponds to that of each point in Fig. 2. The single-component exponential function fittings are for transient signals measured at 15 K (b), 100 K (c) and 280 K (d).

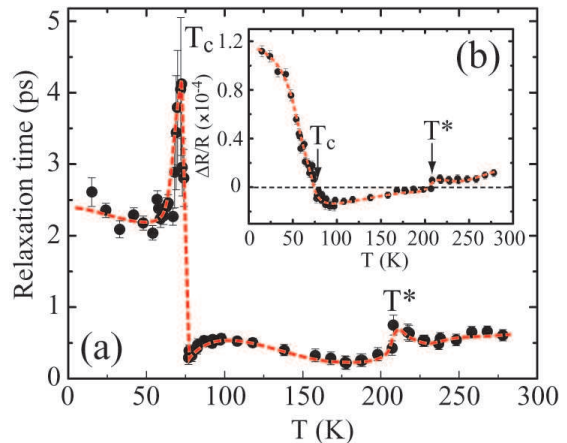


FIG. 2: (Color online) Temperature dependence of (a) the relaxation time of QPs, and (b) the measured amplitude of $\Delta R/R$ derived from the spectra shown in Fig. 1(a). The dashed lines are guides to the eye.

is consistent with previous reports on Y123 [18], but is closely related to that of the probe beam. Below T_c the transient $\Delta R/R$ is independent of the probe polarization and two identical signals are obtained for $\mathbf{E}_{pr}\parallel$ and $\mathbf{E}_{pr}\perp$ ($\mathbf{E}_{pr}\parallel$ and $\mathbf{E}_{pr}\perp$ denoted as the probe polarizations parallel and orthogonal to the b axis of the crystal, respectively). Above T_c , however, the $\Delta R/R$ measured with $\mathbf{E}_{pr}\perp$ is negative while that measured with $\mathbf{E}_{pr}\parallel$ is negligible, which may be owing to the anisotropy of the

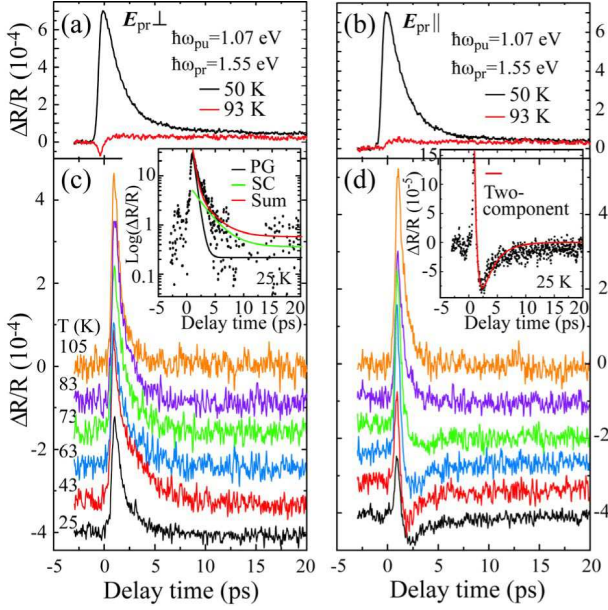


FIG. 3: (Color online) The effect of probe polarization on the signal. The transient $\Delta R/R$ measured at $\hbar\omega_{pu}=1.07$ eV and $\hbar\omega_{pr}=1.55$ eV both below and above T_c with (a) $\mathbf{E}_{pr}\perp$ and (b) $\mathbf{E}_{pr}\parallel$. The transient $\Delta R/R$ measured at $\hbar\omega_{pu}=1.55$ eV and $\hbar\omega_{pr}=1.07$ eV at various temperatures with (c) $\mathbf{E}_{pr}\perp$ and (d) $\mathbf{E}_{pr}\parallel$. For clarity each spectrum except for the topmost one is shifted by 8×10^{-5} . The inset in Fig. 3(c) shows the method used to analyze the signal measured at 25 K. The black line corresponds to single PG-component fitting, the green line to single SC-component fitting and the red line to the sum of the above two fittings. The inset in Fig. 3(d) shows the fitting using a two-component exponential decay function for the signal measured at 25 K (red solid line).

probe transition matrix elements [24].

Further investigations indicate that the transient $\Delta R/R$ also strongly depends on probe energy $\hbar\omega_{pr}$. In Figs. 3(c) and (d) are shown the data measured after exchanging the pump and probe energies used above, i.e. measured at $\hbar\omega_{pu}=1.55$ eV and $\hbar\omega_{pr}=1.07$ eV. For $\mathbf{E}_{pr}\perp$ the sign of $\Delta R/R$ measured at $\hbar\omega_{pr}=1.07$ eV is positive throughout the whole temperature range [Fig. 3(c)]. Above T_c , the one-component exponential decay function $\Delta R/R(T, t)=A(T)\exp(-t/\tau_{PG})$ is used to fit the data well, resulting in the relaxation time $\tau_{PG}\sim 0.5$ ps, which is equal to that measured at $\hbar\omega_{pr}=1.55$ eV in the PG state shown in Fig. 1(c). Since each kind of QP corresponds to one relaxation time, it is natural to assign this component to PG QPs. Below T_c , the signal consists of two components that have slow and fast decays, respectively. In this case, the analysis method is similar to that used in Refs. [14, 15] and illustrated in the inset of Fig. 3(c). We first use a single-component decay function to fit the SC and PG components, respectively, by fixing $\tau_{PG}=0.5$ ps and $\tau_{SC}=2.5$ ps and then obtain a sum of the above two fittings. It can be seen that this method works

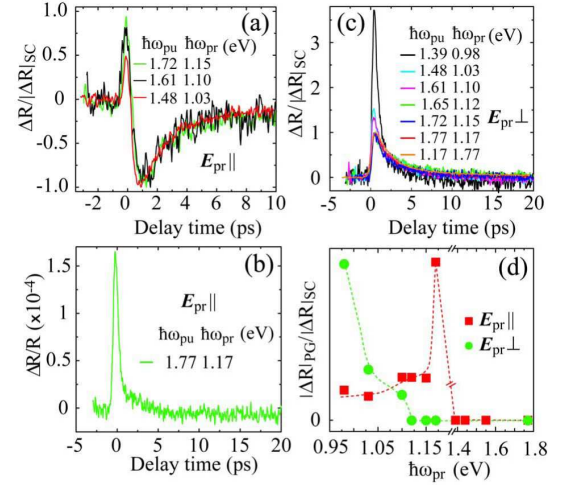


FIG. 4: (Color online) The effect of probe energy on the signal measured at 20 K. (a) Normalized $\Delta R/R$ measured at $\hbar\omega_{pr}$ from 1.03 to 1.15 eV with $\mathbf{E}_{pr}\parallel$. (b) Single PG component measured at $\hbar\omega_{pr}=1.17$ eV with $\mathbf{E}_{pr}\parallel$. (c) Normalized $\Delta R/R$ measured $\hbar\omega_{pr}$ from 0.98 to 1.77 eV with $\mathbf{E}_{pr}\perp$. (d) Probe energy dependence of the amplitude ratio of the PG and SC components. This ratio is helpful in clarifying the change in the PG component with probe energy.

well and we therefore assign the fast-decay component to PG QPs and the slow-decay component to SC QPs. For $\mathbf{E}_{pr}\parallel$ the detected signal consists of two distinct components with opposite signs below T_c , as seen in Fig. 3(d); the fast-decay component is positive and the slow-decay component is negative. A two-component decay function, $\Delta R/R(T, t)=A(T)\exp(-t/\tau_{PG})-B(T)\exp(-t/\tau_{SC})$, is used to obtain a good fit with the data measured below T_c , using parameters of $\tau_{PG}\sim 0.5$ ps and $\tau_{SC}\sim 2.5$ ps. One fitting curve is shown as an example in the inset of Fig. 3(d). With increasing the temperature, the amplitude of the negative component decreases and becomes zero at T_c , suggesting that it originates from SC QPs. Above T_c only the positive component remains whose relaxation time is about 0.5 ps, suggesting that the positive component observed below T_c is due to PG QPs. Therefore, we directly observe the coexistence of PG and SC QPs in UD Bi2212, which have different relaxation dynamics. This time-domain observation of the coexistence of PG and SC QPs below T_c is in good agreement with real-space measurements such as those obtained with scanning tunneling microscopy/spectroscopy (STM/STS) with atomic resolution, which reveal that SC and PG gaps coexist in real space in UD Bi2212 [8, 9, 25]. Here, we would like to emphasize that the coexistence of PG and SC QPs does not mean the “inhomogeneous phase separation” of the PG and SC states in real space. Recent STM/STS results suggest that both the PG and SC QPs should be distributed uniformly for a disorder-free UD Bi2212 sample below T_c [9, 25, 26].

In order to obtain detailed information on the energy dispersion of the charge dynamics of PG and SC QPs below T_c , we further investigate the effect of probe energy on the transient signal at 20 K, indicating that either the PG or SC component can be selectively detected at a specified probe energy. Figure 4(a) shows the signals measured at probe energies of 1.03 to 1.15 eV with $\mathbf{E}_{pr}\parallel$, which is normalized to the amplitude of the SC component to minimize the effect of the pump power on the signal. As is clearly seen, two components originating with SC and PG QPs can be simultaneously detected, as discussed above. More interestingly, with increasing $\hbar\omega_{pr}$ the fraction of PG component increases. At $\hbar\omega_{pr}=1.17$ eV, a single PG component is detected [Fig. 4(b)], i.e. the fraction of PG component in the measured signal is almost 100%. As the probe energy increases further, the PG-component fraction decreases and the SC-component fraction increases and only a single SC component is detected in the energy range from 1.39 to 1.77 eV. To see this trend clearly, we show the amplitude ratio of the PG and SC components $|\Delta R|_{PG}/|\Delta R|_{SC}$ ($|\Delta R|_{SC}$ and $|\Delta R|_{PG}$ corresponds to the amplitudes of the SC and PG components, respectively.) as a function of $\hbar\omega_{pr}$ for $\mathbf{E}_{pr}\parallel$ by solid squares in Fig. 4(d).

The energy dependence of the signal measured with $\mathbf{E}_{pr}\perp$ differs from that measured with $\mathbf{E}_{pr}\parallel$. For $\mathbf{E}_{pr}\perp$ the signal is always positive regardless of $\hbar\omega_{pr}$, as shown in Fig. 4(c). Careful fitting analysis indicates that at $\hbar\omega_{pr}=0.98$ eV the PG component dominates the signal. Increasing the probe energy results in a decrease in the PG component fraction and an increase in the SC component fraction; in the probe energy range from 1.12 to 1.77 eV, only the SC signal is detected. This trend is illustrated in Fig. 4(d) by solid circles, where $|\Delta R|_{PG}$ and $|\Delta R|_{SC}$ are obtained by fitting the data using the method described in the inset of Fig. 3(c). Note that the signals measured at $\hbar\omega_{pr}=1.03$ and 1.10 eV are similar to those measured previously for La214 and Y123 samples [14, 27] that consist of the mixed SC and PG components.

The most important finding of our present investigation is the direct observation of coexisting PG and SC QPs below T_c [Fig. 3(d) and Fig. 4(b)], which agrees well with findings obtained using electronic Raman scattering [1, 2, 3], ARPES [4, 5, 6] and STM/STS [8, 9, 25] that two energy scales coexist below T_c . For UD Bi2212, the SC gap located in nodal regions is distinct from the PG in antinodal regions on the Fermi surface, which suggests that below T_c the PG does not evolve smoothly into the SC gap. As for the time-resolved pump-probe measurement, to our knowledge, it is the first time there has been an unambiguous and direct assignment of the relaxation processes associated with PG and SC QPs based on the sign changes of $\Delta R/R$ at T_c and T^* [Fig. 1(a)], whose relaxation times are ~ 0.5 ps and ~ 2.5 ps, respectively. At

present, however, it is still difficult to infer whether the PG state is a friend or foe of high T_c superconductivity [28].

However, the present investigations clarify an important long-standing puzzle with respect to the sign of the transient $\Delta R/R$ measured by time-resolved optical spectroscopy. We verify that the sign of $\Delta R/R$ depends both on $\hbar\omega_{pr}$ and on the probe beam polarization, which may be due to the anisotropy of the probe transition matrix elements and the inter-band transition probability [24]. Both strongly depend on the probe energy $\hbar\omega_{pr}$ and the band structure of the material [24]. Therefore, a single SC or PG component can be detected separately by tuning the probe polarization and energy. This method for separating the contributions of PG and SC QPs to $\Delta R/R$ is useful for investigating the charge dynamics of QPs in other high- T_c superconductors in order to clarify the universal relationship between the SC and PG states.

This work was supported by the 21st century COE program ‘‘Topological Science and Technology’’ and Grants-in-Aid for Scientific Research from the Ministry of Education, Culture, Sports, Science and Technology, Japan.

Electronic address: yhaoliu@hotmail.com

- [1] M. Opel *et al.*, Phys. Rev. B **61**, 9752 (2000).
- [2] M. Oda, N. Momono and M. Ido, Supercond. Sci. Technol. **13**, R139 (2000); and refereces therein.
- [3] M. Le Tacon *et al.*, Nature Physics **2**, 537 (2006).
- [4] K. Tanaka *et al.*, Science **314**, 1910 (2006).
- [5] T. Kondo *et al.*, Phys. Rev. Lett. **98**, 27004 (2007).
- [6] W. S. Lee *et al.*, Nature **450**, 81 (2007).
- [7] M. Oda *et al.*, J. Phys. Soc. Jpn. **69**, 983 (2000).
- [8] K. McElroy *et al.*, Phys. Rev. Lett. **94**, 197005 (2005).
- [9] A. Hashimoto *et al.*, Phys. Rev. B **74**, 064508 (2006).
- [10] S. D. Brorson *et al.*, Phys. Rev. Lett. **64**, 2172 (1989).
- [11] S. G. Han *et al.*, Phys. Rev. Lett. **65**, 2708 (1990).
- [12] G. L. Easley *et al.*, Phys. Rev. Lett. **65**, 3445 (1990).
- [13] V. V. Kabanov *et al.*, Phys. Rev. B **59**, 1497 (1998).
- [14] J. Demsar *et al.*, Phys. Rev. Lett. **82**, 4918 (1999).
- [15] H. Murakami *et al.*, Europhys. Lett., **60**, 288 (2002).
- [16] N. Gedik *et al.*, Phys. Rev. Lett. **95**, 117005 (2005).
- [17] T. N. Thomas *et al.*, Phys. Rev. B **53**, 12436 (1996).
- [18] C. J. Stevens *et al.*, Phys. Rev. Lett. **78**, 2212 (1997).
- [19] K. Shimatake, Y. Toda, and S. Tanda, Phys. Rev. B **75**, 115120 (2007).
- [20] R. M. Distasil *et al.*, J. Phys. Soc. Jpn. **71**, 1535 (2002).
- [21] G. L. Easley, Phys. Rev. Lett. **51**, 2140 (1983).
- [22] W. Albrecht, *et al.*, Phys. Rev. Lett. **69**, 1451 (1992).
- [23] M. R. Norman *et al.*, Nature **392**, 157 (1998).
- [24] D. Dvorsek *et al.*, Phys. Rev. B **66**, 020510(R) (2002).
- [25] Y. H. Liu *et al.*, Phys. Rev. B **75**, 212507 (2007).
- [26] Y. H. Liu *et al.*, J. Phys. Chem. Solids, in press.
- [27] S. Rast *et al.*, Phys. Rev. B **64**, 214505 (2001).
- [28] M. R. Norman, D. Pines, and C. Kallin, Adv. Phys. **54**, 715 (2005).